Pergamon

Mathl. Comput. Modelling Vol. 19, No. 3/4, pp. 75–88, 1994

0895-7177/94 $6.00 + 0.00

0895-7177(94)E0024-H

An Optimization Procedure for the Design of Prop-Rotors in High Speed Cruise Including the Coupling of Performance, Aeroelastic Stability, and Structures

A. CHATTOPADHYAY AND T. R. MCCARTHY
Department of Mechanical and Aerospace Engineering
Arizona State University, Tempe, AZ, U.S.A.

J. F. MADDEN, III
Rotorcraft Technology Branch
NASA Ames Research Center, Moffett Field, CA, U.S.A.

Abstract—An optimization procedure is developed to address the complex problem of designing prop-rotors in high speed cruise. The objectives are maximization of the aerodynamic efficiency in high speed cruise and minimization of the total rotor weight. Constraints are imposed on aeroelastic stability in cruise and rotor thrust. An isotropic box beam is used to model the principal load carrying member in the blade. Design variables include blade sweep and twist distributions, rotational velocity in cruise, and the box beam wall thickness. Since the optimization problem is associated with multiple design objectives, the problem is formulated using a multiobjective formulation technique known as the Kreisselmeier-Steinhauser function approach. The optimization algorithm is based on the method of feasible directions. A hybrid approximate analysis technique is used to reduce the computational expense of using exact analyses for every function evaluation within the optimizer. The results are compared to two reference rotors, unswept and swept. The optimum result shows significant improvements in the propulsive efficiency in cruise and reductions in the rotor weight without loss of aeroelastic stability or thrust, when compared to the reference unswept rotor. The swept reference rotor is initially unstable and the optimization procedure has been successful in producing a blade design which is fully stable with significant improvements in efficiency and blade weight. Off-design studies performed indicate that the optimum rotor maintains high propulsive efficiency over a wide range of operating conditions.

NOMENCLATURE

c	Nondimensional chord	GJ	Blade torsional rigidity, lb.ft^2
c_0–c_3	Chord distribution parameters	I_θ	Blade polar moment of inertia, slug.ft^2
C_P	Coefficient of total power	k_r	Nondimensional blade radius of gyration
C_T	Coefficient of thrust	L/D	Lift-to-drag ratio
EI_{xx}	Blade lagging stiffness, lb.ft^2	m	Blade mass per unit length, slug/ft
EI_{zz}	Blade flapping stiffness, lb.ft^2	m_0	Nonstructural mass per unit length, slug/ft
$\mathbf{f}_m$	Vector of K-S function constraints	m_1–m_4	Nonstructural mass distribution parameters, slug/ft
$\mathbf{F}_k$	Vector of individual objective functions	SPC	Specific power consumption, lb/m/hp
F_{KS}	Kreisselmeier-Steinhauser objective function		
$\mathbf{g}_j$	Vector of original constraints		

This work was supported by NASA Ames Research Center, under Grant NAG2-771, Technical Monitor, J. F. Madden, III.

SHP	Shaft horse power, hp	α_k	Real part of the k^{th} aeroelastic stability root
p_n	Two-point exponential expansion parameter	$\bar{y}$	Nondimensional radial location, y/R
R	Blade radius, ft	ε_1–ε_3	Sweep distribution parameters
t	Nondimensional box beam wall thickness	η_{ax}	High speed propulsive efficiency
T	Rotor thrust, lb	$\eta_{e\Omega}$	Engine weight efficiency parameter
V_∞	Cruise velocity, knots	Φ	Design variable vector
W	Total rotor weight, lb	λ	Cruise and hover RPM ratio
W_{blade}	Blade structural weight, lb	Λ	Blade sweep, degrees
W_{drive}	Drive system weight, lb	θ	Blade twist, degrees
W_{engine}	Engine weight, lb	θ_1–θ_3	Twist distribution parameters, degrees
W_{fuel}	Fuel weight, lb	ρ	K-S function factor
W_{trans}	Transmission weight, lb	σ	Area-weighted rotor solidity
x, y, z	Reference axes	υ	Minimum allowable blade damping
x_{ac}	Nondimensional aerodynamic lifting line offset	Ω	Rotor RPM

INTRODUCTION

Recently there has been a revival of interest in the development of high speed rotorcraft that demonstrate aerodynamic efficiencies similar to fixed-wing aircraft in high speed cruise while maintaining the acceptable hovering capabilities of helicopters [1]. The design of this class of aircraft is associated with several critical and often conflicting requirements [2–4]. For example, in order to achieve desirable propulsive efficiencies, it is necessary to reduce the tip speed in high speed cruise, which causes the rotor to operate at nonideal rotational velocity [4]. This can be overcome through the use of thin airfoils which have high drag divergence Mach numbers. Thin airfoils, however, have lower maximum lift coefficients, and therefore, in order to produce the required thrust in hover, the rotor solidity must increase. A second approach is to add blade sweep which reduces the effective chordwise Mach numbers. However, swept blades at high speeds demonstrate significant aeroelastic instabilities [5]. The conflicting design requirements also lead to increased drive system weight, which is an important design issue in high speed prop-rotors. The total drive system weight comprises contributions from each of the transmission, the fuel, and the engine weights. The transmission size, and therefore, the weight of the transmission system, is based on the power and torque required. For high speed prop-rotors, since the installed power is governed by cruise conditions, an increase in the high speed cruise requirement results in an increase in the power requirement, which eventually increases the transmission weight. Also, as speed increases, helical tip Mach number limitations result in the need for reduced rotational velocity. Reduction of the rotational speed on a direct shaft driven rotor forces the engine to operate at nonoptimum conditions, thereby increasing the fuel flow in cruise. The reduction in the RPM also make the torque requirement in cruise to be significantly higher than that required in hover [3] resulting in an exponential increase in the drive system design torque, and therefore, in the drive system weight. One way to maintain engine efficiency in cruise is to employ a two-speed gear box to keep the engine rotating at the same optimum speed. However, the two-speed gear box adds complexity and weight to the drive system, thus requiring a design trade-off. Reduction of the engine weight, on the other hand, will reduce the power required, which in turn will make it possible to re-size the engine to a smaller one. Reduction of drive system weight is therefore an important design criterium which can improve the vehicle performance significantly. Reduced structural weight and reduced power requirements lead to increases in specific range and payload delivery efficiency due to reduced fuel consumption. Reduction of power requirements secondarily affects engine size and drive system weight. Finally, a lower empty weight will lead to improved productivity.

Several studies have been performed [6–8] to investigate design trade-offs between the two flight modes. Johnson *et al.* [6] performed a detailed study on the performance, maneuverability, and stability of high speed tilting prop-rotor aircraft, including the XV-15 and the V-22. Liu and McVeigh [7] recently studied the use of highly swept rotor blades for high speed tilt-rotor use. Benoit and Bousquet [8] performed a parametric study to investigate the proper choice of airfoil selection for improved aerodynamic performance. An ideal combination of planform, twist, airfoils, and sweep is necessary to achieve improved aerodynamic performance without introducing substantial weight penalties and aeroelastic instabilities. The use of formal optimization procedures, therefore, seems appropriate in such designs. Although a significant amount of research has been performed in applying these techniques for the design of helicopter rotors [9–11], their application in tilt-rotor designs is relatively new. Recently, Chattopadhyay *et al.* [11–17] have initiated the development of multidisciplinary optimization strategies for addressing this complex aircraft design problem. A first investigation of improving propulsive efficiency with constraints on hover figure of merit, natural frequencies, and stability in cruise was reported by Chattopadhyay and Narayan [12,13]. The problem of minimizing only the drive system weight using aerodynamic design variables such as twist and RPM was addressed by Chattopadhyay *et al.* [14]. An optimization procedure with the coupling of structures and aeroelastic design criteria was presented in [15], where a composite box beam was used to model the load carrying spar inside the airfoil. The use of multiobjective formulation techniques in the design of prop-rotors was demonstrated by McCarthy [16] and McCarthy and Chattopadhyay [17]. Two formal multiobjective function formulation techniques, the Minimum Sum Beta (Min $\Sigma\beta$) [18] and the Kreisselmeier-Steinhauser (K-S) function [19] approaches, were used. The procedure was demonstrated by simultaneously maximizing the propulsive efficiency in high speed cruise and the rotor figure of merit in hover using simplified aerodynamic and structural models.

The purpose of the present paper is to develop a more comprehensive optimum design procedure to address some of the critical design issues in high speed cruise. The propulsive efficiency is maximized and the total rotor weight, which comprises the drive system weight and the blade structural weight, is minimized simultaneously. Constraints are imposed on aeroelastic stability and the rotor thrust in cruise is held constant. Aerodynamic parameters such as blade sweep and twist distributions and rotor RPM are used as design variables. Structural parameters such as nonstructural weights and the box beam wall thickness are included as design variables as well. The Kreisselmeier-Steinhauser (K-S) function approach, which was found to yield better results in [16,17], is used to formulate the multiobjective optimization problem.

MULTIOBJECTIVE OPTIMIZATION PROBLEM

Traditional optimization solution techniques require that only a single objective function be minimized or maximized. In this study, multiple objective functions are chosen; therefore, a multiobjective function formulation technique is required. The technique used is the Kreisselmeier-Steinhauser (K-S) function approach which is described in the following section.

Kreisselmeier-Steinhauser (K-S) Function

The first step in formulating the objective function in this approach involves the transformation of the original objective functions into reduced objective functions [19]. These reduced objective functions assume the following form:

$$\mathbf{F}_k^*(\mathbf{\Phi}) = 1.0 - \frac{\mathbf{F}_k(\mathbf{\Phi})}{F_{k0}} - g_{\max} \leq 0, \qquad k = 1, \ldots, \text{NOBJ}, \tag{1}$$

where $\mathbf{F}_{k0}$ represents the value of the original objective function $\mathbf{F}_k$ calculated at the beginning of each iteration. The quantity $g_{\max}$ is the value of the largest constraint corresponding to the design variable vector $\mathbf{\Phi}$ and is held constant during each iteration. These reduced objective functions

are analogous to constraints, and therefore, a new constraint vector $\mathbf{f}_m(\Phi)$ $(m = 1, 2, \ldots, M$, where M = NCON + NOBJ) is introduced, which includes the original constraints and the constraints introduced by the reduced objective functions (equation (1)). The design variable vector remains unchanged. The new objective function to be minimized is then defined using the K-S function as follows:

$$F_{\mathrm{KS}}(\Phi) = f_{\max} + \frac{1}{\rho} \ln \sum_{m=1}^{M} e^{\rho(\mathbf{f}_m(\Phi) - f_{\max})}, \tag{2}$$

where $f_{\max}$ is the largest constraint corresponding to the new constraint vector $\mathbf{f}_m(\Phi)$ and in general is not equal to $g_{\max}$. The optimization procedure can be explained as follows. When the original constraints are satisfied, the constraints due to the reduced objective functions are violated. Initially, in an infeasible design space where the original constraints are violated, the constraints due to the reduced objective functions (1) are satisfied (i.e., $g_{\max}$ is negative). When this happens, the optimizer attempts to satisfy these constraints, and in doing so, maximizes the original objective functions ($\mathbf{F}_k$). The multiplier ρ is analogous to the draw-down factor of penalty function formulation and controls the distance from the surface of the K-S envelope to the surface of the maximum constraint function. When ρ is large, the K-S function will closely follow the surface of the largest constraint function. When ρ is small, the K-S function will include contributions from all violated constraints.

ANALYSIS AND OPTIMIZATION

In this section, a description of the analysis procedures coupled within the optimization process is provided. This is followed by a description of the optimization procedure.

Structural Analysis

An isotropic, rectangular box beam of equal wall thickness (Figure 1) is used as a perturbational model on an existing prop-rotor blade. The outer dimensions of the box beam are assumed to be fixed percentages of the chord length. The spanwise wall thickness distribution is assumed to vary proportionally with the chord. The structural properties can be calculated based on this model.

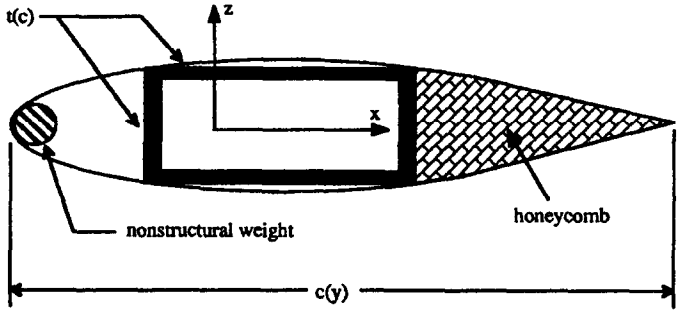

Figure 1. Rotor blade cross-section.

Dynamic, Aerodynamic, and Aeroelastic Analyses

The program CAMRAD/JA [20] is used for blade dynamic, aerodynamic, and aeroelastic stability analyses. A wind tunnel trim option is used and the rotor is trimmed to a specific C_T/σ value (C_T is the coefficient of thrust and σ is the area-weighted solidity of the rotor) using the collective blade pitch. Uniform inflow is assumed since the induced velocity component in high speed cruise is significantly lower than the forward speed of the rotor. The aeroelastic stability analysis is performed using the constant coefficient technique as implemented in CAMRAD/JA.

Fifteen bending degrees of freedom, nine torsional degrees of freedom, and two gimbal degrees of freedom are used for a total of 52 modes. The blade is trimmed within CAMRAD/JA at each optimization cycle so that the intermediate designs, which are feasible designs, represent trimmed configurations.

OPTIMIZATION IMPLEMENTATION

The optimization procedure is based on the method of feasible directions as implemented in the optimization program CONMIN [21]. Since the procedure requires several evaluations of the objective functions and constraints before an optimum design is obtained, the process can be very expensive if full analyses are made for each function evaluation. The objective function and constraints are therefore approximated using a hybrid approximation technique which is described next.

Approximation Technique

The two-point exponential approximation technique [22], which was found to perform well in nonlinear optimization problems [14–17], is used for the approximation of the objective functions and the constraints. This technique takes its name from the fact that the exponent used in the expansion is based upon gradient information from the previous and current design cycles. This technique is formulated as follows:

$$\hat{\mathbf{F}}(\mathbf{\Phi}) = \mathbf{F}(\mathbf{\Phi}_0) + \sum_{n=1}^{\mathrm{NDV}} \left[\left(\frac{\Phi_n}{\Phi_{0n}} \right)^{p_n} - 1.0 \right] \frac{\Phi_{0n}}{p_n} \frac{\partial \mathbf{F}(\mathbf{\Phi}_0)}{\partial \Phi_n}, \tag{3}$$

where $\hat{\mathbf{F}}(\mathbf{\Phi})$ is the approximation of the function $\mathbf{F}(\mathbf{\Phi}_0)$. The approximate values for the constraints, $\hat{\mathbf{g}}_j(\mathbf{\Phi})$, are similarly calculated. The exponent, p_n, is defined by:

$$p_n = \frac{\ln \left\{ \frac{\partial \mathbf{F}(\mathbf{\Phi}_1)}{\partial \Phi_n} \Big/ \frac{\partial \mathbf{F}(\mathbf{\Phi}_0)}{\partial \Phi_n} \right\}}{\ln \left\{ \mathbf{\Phi}_{1n} / \mathbf{\Phi}_{0n} \right\}} + 1.0. \tag{4}$$

The quantity $\mathbf{\Phi}_1$ refers to the design variable vector from the previous iteration, and the quantity $\mathbf{\Phi}_0$ denotes the current design vector. A similar expression is derived for the constraint vector. Equation (4) indicates that in the limiting case of $p_n = 1$, the expansion is identical to the traditional first order Taylor series. When $p_n = -1$, the two-point exponential approximation reduces to the reciprocal expansion form. The exponent is then defined to lie within this interval, such that if $p_n > 1$, it is set identically equal to 1, and if $p_n < -1$, it is set equal to -1. The exponent p_n can then be considered as a "goodness of fit" parameter, which explicitly determines the trade-offs between traditional and reciprocal Taylor series-based expansions, therefore resulting in a hybrid approximation technique.

BLADE MODELING

The formulation and modeling assumptions used in the optimization problem are described in this section.

Aerodynamic Model

The chord, $c(\bar{y})$, twist angle of attack, $\theta(\bar{y})$, and the lifting line offset, $x_{ac}(\bar{y})$, are defined to have the following cubic spanwise distributions:

$$\theta(\bar{y}) = \theta_1(\bar{y} - 0.75) + \theta_2(\bar{y} - 0.75)^2 + \theta_3(\bar{y} - 0.75)^3, \tag{5}$$

$$c(\bar{y}) = c_0 + c_1(\bar{y} - 0.17) + c_2(\bar{y} - 0.17)^2 + c_3(\bar{y} - 0.17)^3, \tag{6}$$

$$x_{ac}(\bar{y}) = \varepsilon_1(\bar{y} - 0.17) + \varepsilon_2(\bar{y} - 0.17)^2 + \varepsilon_3(\bar{y} - 0.17)^3, \tag{7}$$

where θ_1–θ_3, c_0–c_3, and ε_1–ε_3 are the coefficients describing the spanwise variations of twist, chord, and lifting-line offset, respectively. The sweep distribution, $\Lambda(\bar{y})$ is then defined as follows:

$$\Lambda(\bar{y}) = \tan^{-1}\left(\frac{dx}{dy}\right) = \tan^{-1}\left[\varepsilon_1 + 2\varepsilon_2\,(\bar{y} - 0.17) + 3\varepsilon_3\,(\bar{y} - 0.17)^2\right]. \tag{8}$$

The spanwise offset of $\bar{y} = 0.75$ is used in the twist distribution so that the twist is zero at the 75% span location. Note that the parameter c_0 denotes the chord at the hinge offset, $\bar{y} = 0.17$. The hinge offset is used in the lifting line distribution to ensure that zero offset at the blade root. Initially, these parameters are selected to closely model the existing reference blade.

Structural Model

A cubic variation is also assumed for the nonstructural mass distribution, $m_0(\bar{y})$, along blade span,

$$m_0(\bar{y}) = m_1 + m_2(\bar{y} - 0.17) + m_3(\bar{y} - 0.17)^2 + m_4(\bar{y} - 0.17)^3, \tag{9}$$

where m_1–m_4 are the coefficients defining the spanwise distribution. The hinge offset ($\bar{y} = 0.17$) is once again used for the nonstructural mass distribution so that the zeroth order term, m_1, corresponds to a constant nonstructural mass throughout the span, and the higher order terms, m_2–m_4, correspond to spanwise perturbations from this value. These parameters are initially set to values that correspond approximately to 10% of the initial spanwise mass in the existing reference blade.

A box beam perturbational model (Figure 1) is used to calculate the structural properties. The blade stiffness properties are then assumed to vary, from the reference values [23], as follows:

$$\mathrm{EI}_{xx} = f\left(t, c(\bar{y})^4\right), \tag{10}$$

where EI_{xx} is the lagging stiffness, $c(\bar{y})$ is the chord, and t is the box beam wall thickness defined in terms of percent of chord. The flapping stiffnesses (EI_{zz}), the torsional rigidity (GJ), and the polar moment of inertia (I_θ) are defined similarly. The total blade mass and radius of gyration distributions, $m(\bar{y})$ and $k_r(\bar{y})$, respectively, are assumed to vary as follows:

$$m = f\left(t, c(\bar{y})^2\right) + m_0, \tag{11}$$

$$k_r = f\left(t, c(\bar{y})^2\right), \tag{12}$$

where m is the total blade mass comprising the structural and the nonstructural mass.

Because the comprehensive helicopter code CAMRAD/JA models only a straight elastic axis in the dynamic analysis, it is important to include a first approximation of these effects into the equations of motion. In order to more closely model the inertial terms, the polar moment of inertia, I_θ, is updated using the parallel axis theorem as follows:

$$I_\theta = I_\theta + m\,x_{ac}^2. \tag{13}$$

However, it must be noted that the elastic torsion equations, in CAMRAD/JA, are still deficient in modeling high sweep angles. The center of gravity, tension center, and lifting line offsets from the elastic axis are assumed to vary linearly with the chord ratio. Further, the center of gravity calculations also include the effects of the nonstructural weights which are assumed to be located at the 2.5% chord location.

Drive System Model

The drive system weight comprises weight contributions from the engine, the transmission, and the fuel,

$$W_{\text{drive}} = W_{\text{trans}} + W_{\text{fuel}} + W_{\text{engine}}, \tag{14}$$

where the weights are based upon the following empirical formulae:

$$W_{\text{engine}} = 0.12\,\eta_{e\Omega}\,\text{SHP} + 175, \tag{15}$$

$$W_{\text{trans}} = 300\left(1.1\,\frac{\text{SHP}}{\Omega}\right)^{0.8}, \tag{16}$$

$$W_{\text{fuel}} = 1.5\,\text{SPC}\,\text{SHP}, \tag{17}$$

where SHP is the shaft horse power. The specific power consumption (SPC) and the efficiency parameter $\eta_{e\Omega}$ are defined as follows:

$$\text{SPC} = 0.82263 - 1.5168\,\lambda + 1.3933\,\lambda^2 - 0.42269\,\lambda^3, \qquad \text{and} \tag{18}$$

$$\eta_{e\Omega} = 5.7938 - 11.550\,\lambda + 11.235\,\lambda^2 - 3.6399\,\lambda^3, \tag{19}$$

where λ is the rotational velocity ratio defined by

$$\lambda = \left[\frac{\Omega_{\text{cruise}}}{\Omega_{\text{hover}}}\right]. \tag{20}$$

In the above equation, Ω_{cruise} is the rotational velocity in high speed cruise and Ω_{hover} is the rotational velocity in hover. The above expressions are based on generic sizing equations obtained from VASCOMP [24] for the targeted cruise altitude and velocity. Further details can be found in [14].

OPTIMIZATION PROBLEM

The optimization problem addresses the multiple design requirements of maximizing the propulsive efficiency (η_{ax}) and minimizing the total rotor weight (W) simultaneously. The propulsive efficiency is defined as

$$\eta_{ax} = \frac{TV_\infty}{P}, \tag{21}$$

where T is the total rotor thrust, V_∞ is the forward velocity, and P is the total power. The total rotor weight is represented as

$$W = W_{\text{drive}} + 3\,W_{\text{blade}}, \tag{22}$$

where W_{drive} is the drive system weight and W_{blade} is the structural weight of a single blade in the three-bladed rotor.

Since aerodynamic sweep distributions are used as design variables and are therefore altered during optimization, it is important to impose aeroelastic stability constraints to prevent any degradation of the rotor stability in high speed cruise and hover. These constraints take the following form:

$$\alpha_k \leq -\upsilon, \qquad k = 1, 2, \ldots, \text{NMODE}, \tag{23}$$

where NMODE is the total number of modes considered in cruise and α_k is the real part of the stability root. The quantity υ denotes the minimum allowable blade damping and is defined to be a small positive number. It is also important to ensure that the rotor thrust is maintained during the optimization process. However, since the rotor is trimmed to a specific C_T/σ value, and the solidity, σ, is not altered during optimization, the rotor maintains constant thrust throughout the optimization process.

Design Variables

At high Mach numbers, the twist has a significant effect on the cruise efficiency. It also plays an important role in hover. Therefore, the twist distribution is used as a design variable. A cubic twist distribution is chosen to provide the optimizer with more flexibility, and the coefficients θ_1–θ_3 that define the spanwise distribution are used as design variables. Similarly, the parameters that define the blade sweep (ε_1–ε_3) are also selected as design variables. The rotational velocity Ω in high speed cruise plays a significant role in the total drive system weight calculations, and is therefore selected as a design variable. Finally, the parameters that define the nonstructural weight distribution (m_1–m_4) and the nondimensional box beam wall thickness t are also selected as design variables.

RESULTS

The rotor used as a reference is an advanced three-bladed prop-rotor with a gimballed hub. The blade radius is 12.5 feet. The rotor was designed for a cruise speed of 300 knots. The blade is discretized into 51 structural stations and 21 aerodynamic stations. A total of 52 stability modes (NMODE) are considered. Using a wind tunnel trim option, the optimum rotor is trimmed to a C_T/σ value of 0.0432 that corresponds to an aircraft lift-to-drag ratio (L/D) of 8.4. This, along with the fact that the solidity σ of the rotor is held fixed during optimization, ensures that the optimized rotor retains the same thrust as the reference configuration (825 lbs.). The optimization is performed at a cruise velocity of 400 knots at an altitude of 25,000 feet above sea level. For the calculation of the drive system weight, a reference rotor RPM = 570 is used. A uniform inflow model is used. Two initial conditions are used as baseline configurations. The first reference blade corresponds to the existing prop-rotor with zero sweep [23]. The second configuration corresponds to an initially swept blade. The flight conditions are summarized in Table 1. The K-S function approach is found to be efficient, and smooth convergence to the optimum blade is obtained in 22 cycles.

Table 1. Flight conditions.

Forward velocity, V_∞	400 knots
C_T/σ	0.0432
Aircraft L/D	8.4
Rotor thrust	825 lbs
Altitude	25000 ft
Blade radius	12.5
Reference RPM (cruise)	421 RPM
Reference RPM (hover)	570 RPM

The optimum results are presented in Table 2 and Figures 2–12. Table 2 and Figure 2 show that the propulsive efficiency (η_{ax}) is significantly increased from reference to optimum. Large reductions are also obtained in the total rotor weight (W). The optimum blade represents a 5.53% increase in the propulsive efficiency and a 3.49% reduction in the total rotor weight from the unswept reference blade. Although the propulsive efficiency of the reference swept blade is 4.04% greater and the total rotor weight is 2.31% lower than the unswept reference blade, the blade is highly unstable initially. The optimization process yields a blade with a 1.43% increase in η_{ax} and a 1.21% decrease in the total weight from the swept reference blade. The individual weight components are shown in Figure 3, which indicates that the reduction in the total rotor weight, in the optimum rotor, is attributable to the large reduction in the drive system weight (W_{drive}). For the optimum rotor, W_{drive} is reduced by 7.75% from the reference unswept blade, whereas the individual blade structural weight (W_{blade}) is actually increased by 7.81%. The reduction in the drive system weight is due to the increased rotational velocity of the rotor

(RPM), as shown in Table 2, and the increased propulsive efficiency. The blade structural weight increases in order to satisfy the aeroelastic stability through the addition of nonstructural masses at the chord tip and the increase in the stiffness in the optimum blade.

Table 2. Summary of optimum results.

	Unswept	Swept	Optimum
Objective functions			
η_{ax}	0.799	0.831	0.843
W (lb)	2492	2434	2405
W_{drive} (lb)	1809	1752	1669
W_{blade} (lb)	227.5	227.5	245.2
RPM	421	421	452

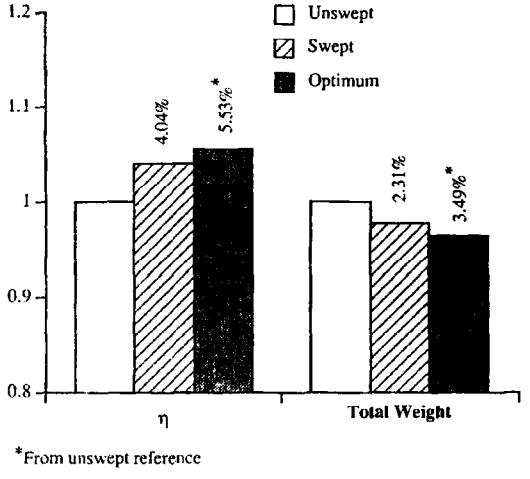

Figure 2. Comparison of optimum results.

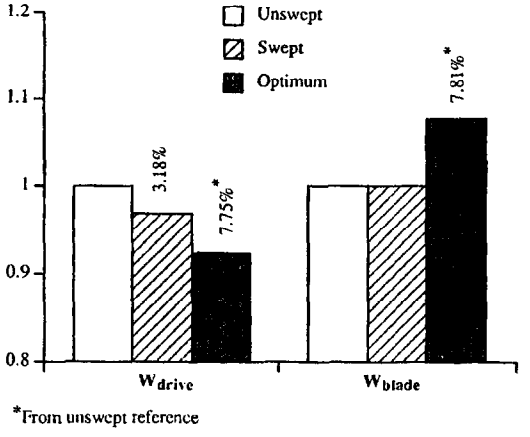

Figure 3. Comparison of individual weights.

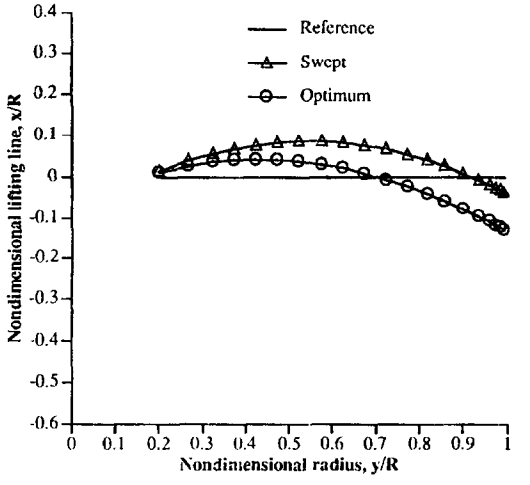

Figure 4. Spanwise lifting line offset, x_{ac}, distribution.

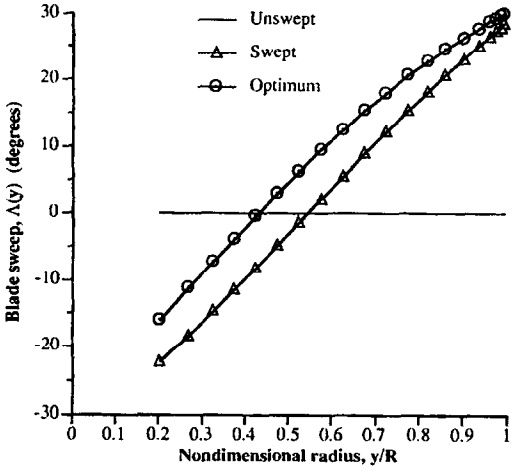

Figure 5. Spanwise blade sweep, $\Lambda(y)$, distributions.

The blade lifting line offset (x_{ac}) and sweep (Λ) distributions are presented in Figures 4 and 5. From Figure 4, it is seen that the reference swept rotor and the optimum rotor are initially swept forward near the root and swept backward outboard of midspan. The swept reference rotor has

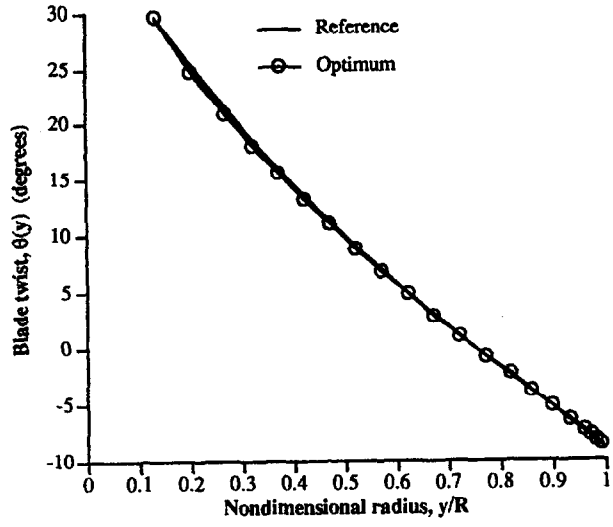

Figure 6. Spanwise blade twist, $\theta(y)$, distributions.

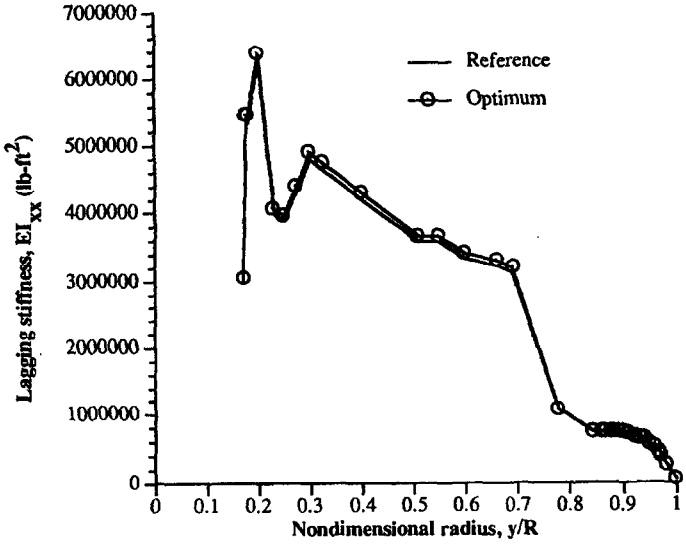

Figure 7. Spanwise lagging stiffness, EI_{xx}, distributions.

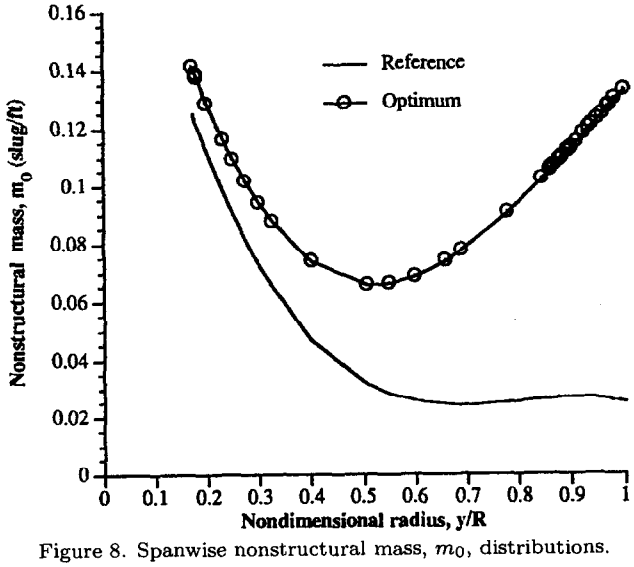

Figure 8. Spanwise nonstructural mass, m_0, distributions.

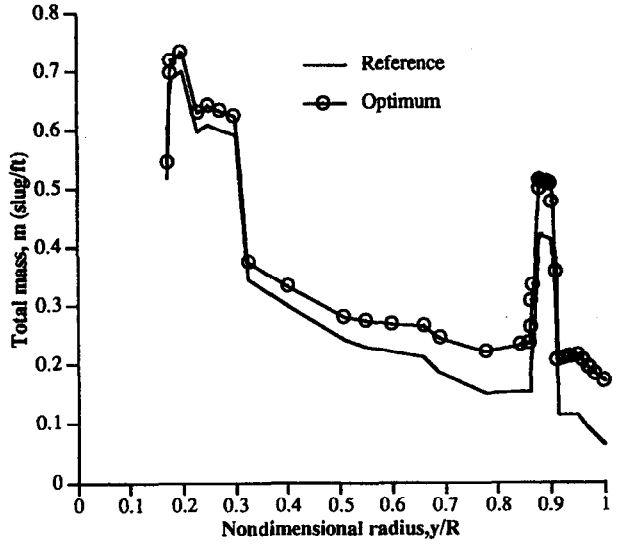

Figure. 9 Spanwise total mass, m, distributions.

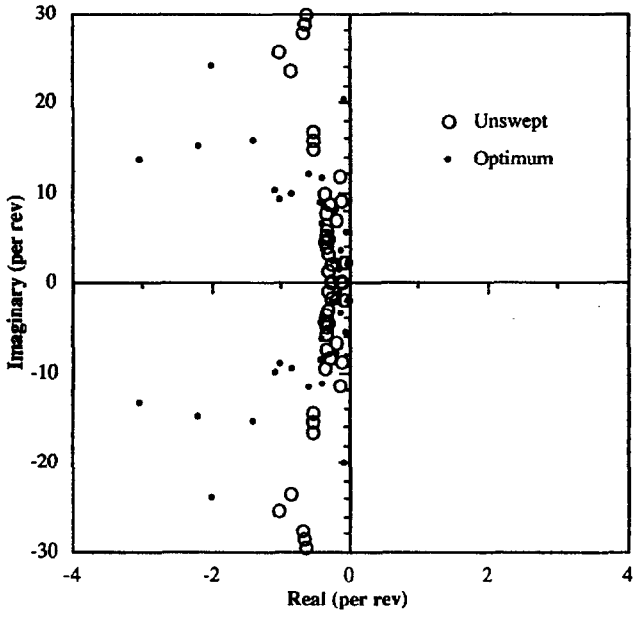

Figure 10. Comparison of unswept reference rotor and optimum rotor aeroelastic stability roots.

more forward sweep than the optimum rotor, and similarly, the optimum rotor is swept further backwards. However, from Figure 5, it is seen that although the optimum rotor has a greater lifting line offset at the tip than the swept reference rotor, only a small increase is obtained in the actual magnitude of the blade sweep angle (equation (8)). The reason for the increase in the aft sweep is two-fold. First, the increase in backward sweep increases the aerodynamic performance, which increases the propulsive efficiency and decreases the drive system weight. Second, by increasing the sweep near the tip, the effective Mach number is reduced, which allows for an increase in the rotor RPM which further decreases the drive system weight.

The blade twist distributions for the reference and the optimum rotors are shown in Figure 6. Since the twist distributions are identical in both the reference unswept and swept configurations, both the reference configurations will be referred to as the reference blade in the following discussions. Figure 6 indicates slight changes in the twist distributions, notably near the blade

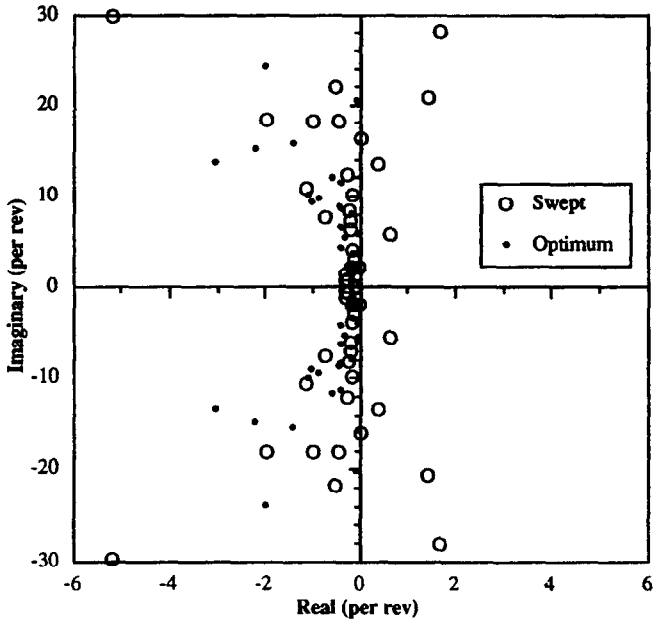

Figure 11. Comparison of swept reference rotor and optimum rotor aeroelastic stability roots.

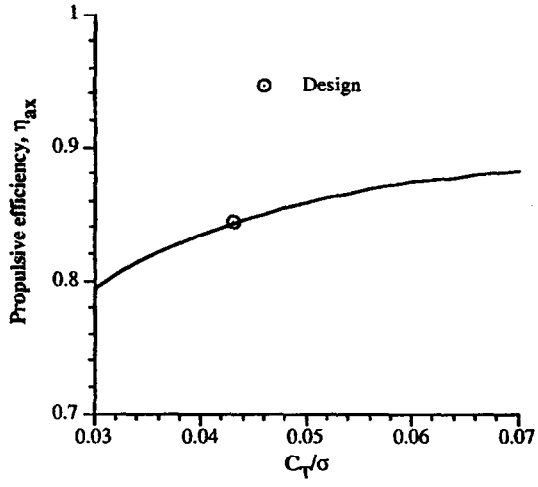

Figure 12. Off-design performance of optimized blade.

root (approximately a 0.6° reduction in blade twist from reference to optimum). This can be explained by noting that the reference twist distribution represents an existing distribution for an advanced prop-rotor and therefore is very efficient initially.

The blade stiffnesses are slightly increased during the optimization process. As a typical representation of these stiffnesses, the lagging stiffness (EI_{xx}) of the reference and the optimum rotors are shown in Figure 7. However, significant changes are observed in the nonstructural mass m_0 and the total blade mass m distributions as shown in Figures 8 and 9. Figure 8 shows that the nonstructural mass is only slightly increased near the root, but is significantly increased at the tip. The result of this larger nonstructural mass increment is manifested in the total mass distribution (Figure 9) where again slight increases are seen near the root and large increases are found at the outboard locations. The reason for the nonstructural mass increase at outboard locations is to move the center of gravity forward in order to stabilize the blade. By stabilizing the blade in this manner, rather than by increasing the stiffness, the optimizer is primarily adding weight only at the outboard locations, thereby avoiding weight penalties throughout the blade span. This has the desired overall effect of maintaining the blade weight at a minimum value.

The aeroelastic stability roots are seen in Figures 10 and 11. Figure 10 presents the stability roots of the reference unswept rotor and the optimum rotor indicating that aeroelastic stability is maintained after optimization. Figure 11 shows that the swept reference rotor is initially highly unstable with sizable unstable roots. The optimization procedure has been successful in producing a fully stable design.

The optimization is performed in cruise for a specific value of thrust which corresponds to a specific value of the nondimensional thrust coefficient, C_T/σ. Therefore, in order to investigate the performance characteristics of the optimum rotor at "off-design" points, the propulsive efficiency η_{ax} is evaluated at several different values of C_T/σ. Figure 12 presents the propulsive efficiency for these off-design points and shows that the optimum rotor maintains high values of η_{ax} over a wide range of C_T/σ. This indicates that the performance of the optimum rotor does not deteriorate at off-design points and even increases for higher values of C_T/σ.

CONCLUSIONS

An efficient optimization procedure has been developed for the synthesis and design of prop-rotors in high speed cruise. Results are obtained with the integration of aerodynamic performance, aeroelastic, and structural design criteria. The propulsive efficiency is maximized and the total rotor weight is minimized simultaneously. The rotor weight comprises the blade structural weight and the drive system weight. Constraints are imposed on the real part of the aeroelastic stability roots. The Kreisselmeier-Steinhauser function is used to formulate the multiobjective problem into a single composite objective function. The optimization algorithm used consists of a nonlinear programming technique coupled with an approximate analysis procedure. The results obtained are compared to two reference blades, unswept and swept. The following observations are made from this study.

(1) The optimization algorithm yielded a significant increase in the propulsive efficiency and a significant decrease in the total rotor weight. The large reductions in the drive system weight are caused by the increase in the rotor RPM and cruise efficiency.
(2) The optimum rotor was efficiently stabilized from an initially unstable design.
(3) The optimum blade was swept in the backward direction to improve efficiency, decrease the effective tip Mach number, and improve the aeroelastic stability.
(4) The nonstructural mass was increased throughout the blade span, more significantly near the blade tip, to satisfy the aeroelastic stability constraints without incorporating a total rotor weight penalty.

REFERENCES

1. P. Talbot, J. Phillips and J. Totah, Selected design issues of some high speed rotorcraft concepts, Presented at the *AIAA/AHS/ASEE Aircraft Design, Systems and Operations Conference*, Dayton, OH, September 17–19, 1990.
2. J.B. Wilkerson, J.J. Schneider and K.M. Bartie, Technology needs for high speed rotorcraft (1), NASA CR 177585, (May 1991).
3. M.W. Scott, Technology needs for high speed rotorcraft (2), NASA CR 177590, (August 1991).
4. J. Rutherford, M. O'Rourke, C. Martin, M. Lovenguth and C. Mitchell, Technology needs for high speed rotorcraft, NASA CR 177578, (April 1991).
5. M.W. Nixon, Parametric studies for tilt-rotor aeroelastic stability in high-speed flight, AIAA Paper No. 92-2568, In *Proceedings of the 33rd AIAA/ASME/ASCE/AHS Structures, Structural Dynamics, and Materials Conference*, Dallas, TX, April 13–15, 1992.
6. W. Johnson, B.H. Lau and J.V. Bowles, Calculated performance, stability, and maneuverability of high speed tilting prop-rotor aircraft, *Vertica* **11** (1987).
7. J. Liu and M.A. McVeigh, Design of swept blade rotors for high-speed tilt-rotor application, Paper No. AIAA 91-3147, Presented at the *AIAA Aircraft Design Systems and Operations Meeting*, Baltimore, MD, September 23–25, 1991.
8. B. Benoit and J.M. Bousquet, Aerodynamic design of a tilt-rotor blade, Presented at the *17th ICAS Congress*, Stockholm, Sweden, September 9–14, 1990.

9. R. Celi and P.P. Friedmann, Structural optimization with aeroelastic constraints of rotor blades with straight and swept tips, *AIAA Journal* **28** (5), 928–936 (May 1990).
10. J.W. Lim and I. Chopra, Aeroelastic optimization of a helicopter rotor, *Proceedings of the 44^{th} Annual Forum of the American Helicopter Society*, Washington, DC, June 1988, pp. 545–558.
11. T.R. McCarthy and A. Chattopadhyay, Multidisciplinary optimization of helicopter rotor blades including design variable sensitivity, Presented at the *Fourth AIAA/USAF/NASA/OAI Symposium on Multidisciplinary Analysis and Optimizations*, Cleveland, OH, September 1992.
12. A. Chattopadhyay and J. Narayan, Optimum design of high speed prop-rotors using a multidisciplinary approach, Presented at the *48^{th} Annual Forum of the American Helicopter Society*, Washington DC, June 3–5, 1992.
13. A. Chattopadhyay and J. Narayan, A design optimization procedure for high speed prop-rotors, AIAA Paper No. 92-2375, In *Proceedings of the 33^{rd} AIAA/ASME/ASCE/AHS Structures, Structural Dynamics, and Materials Conference*, Dallas, TX, April 13–15, 1992.
14. A. Chattopadhyay, T.R. McCarthy and J.F. Madden, A design optimization procedure for minimizing drive system weight of high speed prop-rotors, Presented at the *4^{th} AHS Specialists Meeting on Multidisciplinary Optimization*, Atlanta, GA, April 26–28, 1993.
15. A. Chattopadhyay, T.R. McCarthy and J.F. Madden, Structural optimization of high speed prop-rotors including aeroelastic stability constraints, *Mathl. Comput. Modelling* **18** (3/4), 101–114 (1993).
16. T.R. McCarthy, An integrated multidisciplinary optimization approach for rotary wing design, Masters Thesis, Arizona State University, (December 1992).
17. T.R. McCarthy and A. Chattopadhyay, Design of high speed prop-rotors using multiobjective optimization techniques, AIAA Paper No. 93-1032, In *Proceedings of the 1993 AIAA/AHS/ASEE Aerospace Design Conference*, Irvine, CA, February, 1993.
18. W.H. Weller and M.W. Davis, Application of design optimization techniques to rotor dynamics problems, In *Proceedings of the 42^{nd} Annual Forum of the AHS*, Washington, DC, June 2–4, 1986, pp. 27–44.
19. J. Sobieszczanski-Sobieski, A. Dovi and G. Wrenn, A new algorithm for general multiobjective optimization, NASA TM-100536, (March 1988).
20. W. Johnson, *A Comprehensive Analytical Model of Rotorcraft Aerodynamics and Dynamics—Johnson Aeronautics Version*, Vol. II: User's Manual.
21. G.N. Vanderplaats, CONMIN—A FORTRAN program for constrained function minimization, *User's Manual*, NASA TMX-62282, (July 1987).
22. G.M. Fadel, M.F. Riley and J.M. Barthelemy, Two point exponential approximation method for structural optimization, *Structural Optimization* **2**, 117–224 (1990).
23. S. Lamon, XV-15 advanced technology blade, ultimate stress analysis, Boeing Report Number D210-12345-1, (1985).
24. A.H. Schoen *et al.*, *User's Manual for VASCOMP II, The VISTOL Aircraft Sizing and Performance Computer Program*, Report d8-0375, Volume IV, Boeing Vertol Company, (1980).